

# An Accurate AoA Estimation Approach for Indoor Localization Using Commodity Wi-Fi Devices

Hao-Xiang Chen, Bin-Jie Hu\*, Li-Li Zheng, Zong-Heng Wei

School of Electronic and Information Engineering

South China University of Technology

Guangzhou, China

e-mail: scut-chen@foxmail.com, eebjiehu@scut.edu.cn, zll\_scut@163.com, wei.zongheng@mail.scut.edu.cn

**Abstract**—Angle-of-Arrival (AoA) is one of the important indoor localization techniques. In this paper, we study on the AoA-based indoor localization by using commodity Wi-Fi devices. However, most existing AoA-based localization approaches face a critical challenge, those accuracies of AoA estimation are degraded when the Signal-to-Noise Ratio (SNR) becomes low. To solve this problem, we propose CSI forward/backward smoothing algorithm to improve the performance of AoA estimation. Experimental results show that our approach can efficiently mitigate AoA estimation accuracy deterioration at low SNRs and achieve higher localization accuracy compared with existing AoA-based localization approach in reality.

**Keywords**—AoA; Wi-Fi; CSI forward/backward smoothing

## I. INTRODUCTION

With the development of Internet of Thing (IoT), location information has become a crucial component of many IoT applications [1]. Unlike outdoor environments, Global Positioning System (GPS) fails in indoor environments because GPS signals cannot penetrate building materials. Therefore, how to achieve accurate indoor localization based on commodity infrastructure is an urgent problem for academic and industrial.

Due to the ubiquity of Wi-Fi infrastructure, Wi-Fi-based indoor localization technology is the mainstream solution to the above problem in academic. At present, most of the Wi-Fi-based solutions are using fingerprinting approaches [2-5], which will be easy to implemented. When the fingerprint database is constructed in off-line stage, they can achieve meter-level localization accuracy in on-line stage. As is known to all, the disadvantage of fingerprinting-based approaches is that the fingerprint database construction takes a lot of time and resources. Moreover, when the environment changes, we need to reconstruct the fingerprint database, otherwise the performance of localization will be deteriorated significantly.

Comparing with fingerprinting-based approaches, Angle-of-Arrival (AoA) based approaches have attracted widely attention due to their zero start-up costs. Recently, multi-antenna has been deployed in the commodity Wi-Fi infrastructure, which allows us to perform AoA-based indoor localization approaches via Wi-Fi.

As far as we know, CUPID [6] is the first system that implements AoA-based localization using commodity Wi-Fi devices. It employs the *multiple signal classification* (MUSIC) [7] algorithm for AoA estimation to achieve meter-level

localization accuracy without any additional overhead. However, this system only has three antennas, so that the multipath cannot be effectively resolved by the MUSIC algorithm, resulting in poor localization accuracy. ArrayTrack [8] employs eight antennas to improve the robustness of the MUSIC algorithm in indoor environment, which can be implemented on the WARP radio platform and can achieve sub-meter localization accuracy. However, due to the large number of antennas, it is difficult to apply to commercial Wi-Fi devices. SpotFi [9] proposes the joint AoA and Time-of-Flight (ToF) estimation algorithm to estimate the parameters precisely for each path even when the Access Point (AP) only equipped with three antennas. It overcomes the disadvantage of the ArrayTrack and can be implemented on commodity Wi-Fi devices. In the case of LOS, SpotFi can achieve a median localization error of 40cm. However, in practice, SpotFi faces a crucial challenge. In the case of low SNRs, the performance of the joint AoA and ToF estimation algorithm proposed by SpotFi will decrease, which eventually lead to a poor localization accuracy. Note that this situation occurs frequently in a complex indoor environment. Unfortunately, it is difficult to increase the SNR at the receiver when the Wi-Fi transmit power is limited. To address this problem, we propose the CSI forward/backward smoothing algorithm to improve the joint AoA and ToF estimation algorithm proposed by SpotFi, which can provide reliable AoA and ToF estimation at low SNRs.

The rest of the paper is organized as follow. In Section II, we give the relevant background knowledge of the AoA and ToF estimation. In Section III, we propose the CSI forward/backward smoothing for the joint AoA and ToF estimation and show the performance through simulation. Section IV introduces the other three modules of our localization system. The experimental results are demonstrated in Section V. Finally, we summarize the full text in Section VI.

## II. BACKGROUND AND MOTIVATION

SpotFi [9] is the state-of-the-art AoA-based localization system. And to understand the limitation of it, we begin with the basics of relevant theory.

### A. Basics of Joint AoA-ToF Estimation

There are two typical parameters for each propagation path corresponding to the receiver, i.e., AoA and ToF. Considering the signal reaches the receiver from a propagation path, on the one hand, if the receiver is equipped with a multi-antenna uniform linear array, the AoA will generate a corresponding

\* Corresponding author

Email address: eebjiehu@scut.edu.cn (Bin-Jie Hu)

phase shift across the antennas, as shown in Figure 1. Intuitively, let  $\theta$  denote the AoA, relative to the first antenna, the phase shift generated at the  $m^{th}$  antenna is  $e^{-j2\pi f(m-1)d\frac{\sin\theta}{c}}$ , where  $f$  is the frequency of signal and  $c$  is the speed of light. In general, in order to achieve the best performance of the AoA estimation,  $d = \lambda/2$ , where  $\lambda$  is the wavelength of signal. On the other hand, there is no doubt that the ToF will also produce a phase shift across subcarriers when the transceiver is based on Orthogonal Frequency Division Multiplexing (OFDM) technology to communicate. Relative to the first subcarrier, the phase shift generated at the  $k^{th}$  subcarrier is  $e^{-j2\pi(k-1)\Delta f\tau}$ , where  $\Delta f$  is the frequency interval of two consecutive subcarriers and  $\tau$  is the ToF.

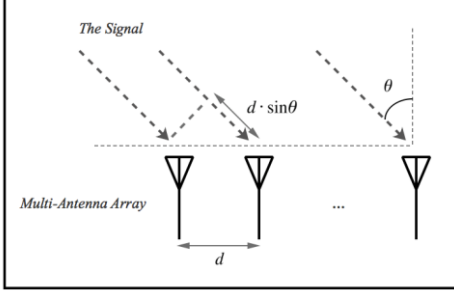


Fig. 1. The model of AoA estimation.

In an indoor environment, assuming that there are  $L$  propagation paths, we employ  $K$  subcarriers to transmit data and the receiver equipped with  $M$  antennas. According to the above, the received signal containing all propagation paths can be expressed as:

$$X = A \cdot F + N \quad (1)$$

where  $X$  is the received signal matrix at the receiver,  $F$  is the vector of path coefficient, and  $N$  is the vector of noise. It is worth noting that  $A$  is the steering matrix, which contains  $L$  steering vectors, represented as follows:

$$A = [\alpha(\theta_1, \tau_1), \dots, \alpha(\theta_l, \tau_l), \dots, \alpha(\theta_L, \tau_L)] \quad (2)$$

where  $\alpha(\theta_l, \tau_l)$  is the steering vector of the  $l^{th}$  propagation path, which consists of a series of phase shifts corresponding to all subcarriers at all antennas generated by the AoA  $\theta_l$  and ToF  $\tau_l$  of the propagation path  $l$ . So  $\alpha(\theta_l, \tau_l)$  is denoted by:

$$\alpha(\theta_l, \tau_l) = [\alpha_{1,1}(\theta_l, \tau_l), \dots, \alpha_{m,k}(\theta_l, \tau_l), \dots, \alpha_{M,K}(\theta_l, \tau_l)] \quad (3)$$

Intuitively, for the  $k^{th}$  subcarrier at  $m^{th}$  antenna, the phase shift  $\alpha_{m,k}(\theta_l, \tau_l)$  can be expressed as follows:

$$\alpha_{m,k}(\theta_l, \tau_l) = e^{-j2\pi[f(m-1)d\frac{\sin\theta}{c} + (k-1)\Delta f\tau]} \quad (4)$$

After the steering matrix  $A$  is constructed, we calculate the covariance matrix of the  $X$ , i.e.,  $R = XX^H$ . Finally, we employ MUSIC algorithm [7] to jointly estimate AoA and ToF. The basic idea of MUSIC is that the steering vectors in  $A$  are orthogonal to eigenvectors of  $R$  corresponding to the eigenvalue zero. As a result, we can estimate the AoAs and ToFs for all propagation paths by searching the peak of MUSIC pseudo-spectrum.

In our implementation, the receiver is equipped with three antennas and an Intel 5300 NIC, so that the Channel State Information (CSI) can be obtained through Linux CSI Tool

[11]. The firmware reports the CSI of 30 subcarriers at each antenna. Therefore, in our system, the CSI matrix can be expressed as:

$$CSI = \begin{bmatrix} csi_{1,1} & csi_{1,2} & \dots & csi_{1,30} \\ csi_{2,1} & csi_{2,2} & \dots & csi_{2,30} \\ csi_{3,1} & csi_{3,2} & \dots & csi_{3,30} \end{bmatrix} \quad (5)$$

where  $csi_{m,k}$  represents the CSI of  $k^{th}$  subcarrier at  $m^{th}$  antenna. Note that each CSI value can be regarded as a received signal at the receiver, so the CSI matrix is equivalent to the received signal matrix  $X$  mentioned above. Undoubtedly, using the above joint estimation algorithm to the CSI matrix, we can easily obtain the AoAs and ToFs of all propagation paths.

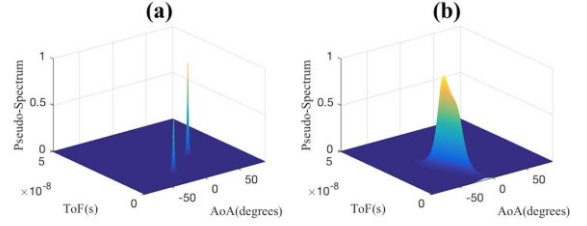


Fig. 2. The results of Simulation 1.

### B. Basics of CSI Smoothing

In the previous section, to simplify the discussion, we temporarily ignored the constraints of MUSIC [7]. Theoretically, to ensure that the MUSIC algorithm works effectively, the covariance matrix  $R$  must be guaranteed to be full rank. In a typical indoor environment, the signal arrives at the receiver through multiple propagation paths. Since the signals from different propagation paths have the same frequency, they are coherent. This will cause the covariance matrix  $R$  to become a singular matrix, which will lead to the MUSIC algorithm failure eventually [10].

To address this problem in practice, SpotFi [9] applies the spatial smoothing [10] to the CSI matrix to perform *CSI smoothing*, then obtains a new measurement matrix  $X$  called *smoothed CSI matrix*. For more details, please refer to section 3.1.2 of [9]. After that, the AoA and ToF of the propagation path will be estimated using the MUSIC algorithm.

However, the indoor environment is complicated. There are many cases where the SNR is not high in Wi-Fi communication process. At this time, the effectiveness of the CSI smoothing proposed by SpotFi will be degraded and lead to a poor AoA and ToF estimation. In order to prove our argument, we conducted a simulation called Simulation 1.

In the Simulation 1, we assumed that both the transmitter and the receiver operates in the 5.2GHz band with SNR of 20db, which is not a high SNR value in Wi-Fi communication. The receiver equipped with three antennas and the spacing of antenna is  $\lambda/2$ . The interval of two consecutive subcarriers is 1.25MHz. First of all, we set up two coherent signals with the AoA  $-20^\circ$ ,  $30^\circ$  and ToF 10ns, 20ns respectively. Figure 2(a) shows the result of the joint AoA and ToF estimation based on MUSIC using CSI smoothing, clearly, which can distinguish two peaks of MUSIC pseudo-spectrum. However, when we set up another two coherent signals with the AoA  $-20^\circ$ ,  $-30^\circ$  and ToF 10ns, 20ns, unfortunately, as shown in the Figure 2(b), it can not distinguish two peaks using CSI smoothing in the case of 20db SNR.

According to the results of Simulation 1, we believe that if two propagation paths are close to each other, i.e., the AoAs and ToFs of the two propagation paths are similar, we will fail to distinguish these two signals by the MUSIC algorithm after using CSI Smoothing at low SNRs.

### III. CSI FORWARD/BACKWARD SMOOTHING

To improve the joint AoA and ToF estimation performance of the MUSIC algorithm at low SNRs, we must solve the problem which discussed in previously. Referring to the idea of [12], we propose CSI forward/backward smoothing to achieve this goal. In the rest of this section, we will elaborate on the details of our algorithm and verify the performance of it by simulation.

In the section 3.1.2 of SpotFi [9], the authors have shown that the CSI values at different subarrays obtained by shifting a fixed subset of the CSI matrix can be written as a linear combination of the same steering matrix. According to this observation, the CSI forward/backward smoothing will be easy to understand.

$$CSI = \begin{bmatrix} csi_{1,1} & \cdots & csi_{1,15} & csi_{1,16} & \cdots & csi_{1,30} \\ csi_{2,1} & \cdots & csi_{2,15} & csi_{2,16} & \cdots & csi_{2,30} \\ csi_{3,1} & \cdots & csi_{3,15} & csi_{3,16} & \cdots & csi_{3,30} \end{bmatrix}$$

Fig. 3. CSI forward smoothing.

In our implementation, Intel 5300 NIC reports CSI matrix, i.e.,  $X$ , with size  $3 \times 30$ . In order to construct the smoothed CSI matrix from CSI matrix using CSI forward/backward smoothing, let's assume that the size of the fixed subset is  $2 \times 15$ , which means that one of subarrays contains 30 CSI values, including 15 subcarriers at 2 antennas. For clarity, we divide CSI forward/backward smoothing into two stages: CSI forward smoothing and CSI backward smoothing. In the CSI forward smoothing stage, we start shifting the fixed subset from the first 15 subcarriers at the first two antennas of the CSI matrix and try all possible shifts, so that we can obtain 32 different CSI subarrays. This process is shown in the Figure 3, where the red dotted box denotes the size of the fixed subset and the initial position of shifting, and the red dotted arrow indicates the direction of shifting. We note that the CSI forward smoothing is the same as the CSI smoothing in SpotFi [9] and is as part of our method. In the CSI backward smoothing stage, at first, we perform complex conjugate on all CSI values of the CSI matrix denoted as:

$$CSI^* = \begin{bmatrix} csi_{1,1}^* & csi_{1,2}^* & \cdots & csi_{1,30}^* \\ csi_{2,1}^* & csi_{2,2}^* & \cdots & csi_{2,30}^* \\ csi_{3,1}^* & csi_{3,2}^* & \cdots & csi_{3,30}^* \end{bmatrix} \quad (6)$$

then we start to shifting the fixed subset. On the contrary, as shown in the Figure 4, we start shifting the fixed subset from the last 15 subcarriers at the last two antennas of the CSI conjugate matrix, i.e.,  $CSI^*$ , and try all possible shifts to obtain another 32 different CSI subarrays as usual.

$$CSI^* = \begin{bmatrix} csi_{1,1}^* & \cdots & csi_{1,15}^* & csi_{1,16}^* & \cdots & csi_{1,30}^* \\ csi_{2,1}^* & \cdots & csi_{2,15}^* & csi_{2,16}^* & \cdots & csi_{2,30}^* \\ csi_{3,1}^* & \cdots & csi_{3,15}^* & csi_{3,16}^* & \cdots & csi_{3,30}^* \end{bmatrix}$$

Fig. 4. CSI backward smoothing.

After these two stages, we obtain a total of 64 different CSI subarrays with the same steering matrix  $A$ , thus, the structure of smoothed CSI matrix can be deduced easily, as shown in the Figure 5.

$$\begin{bmatrix} csi_{1,1} & csi_{1,2} & \cdots & csi_{1,16} & csi_{2,1} & \cdots & csi_{2,16} & csi_{3,30}^* & csi_{3,29}^* & \cdots & csi_{3,15}^* & csi_{2,30}^* & \cdots & csi_{2,15}^* \\ csi_{1,2} & csi_{1,3} & \cdots & csi_{1,17} & csi_{2,2} & \cdots & csi_{2,17} & csi_{3,29}^* & csi_{3,28}^* & \cdots & csi_{3,14}^* & csi_{2,29}^* & \cdots & csi_{2,14}^* \\ \vdots & \vdots & \vdots & \vdots & \vdots & \vdots & \vdots & \vdots & \vdots & \vdots & \vdots & \vdots & \vdots & \vdots \\ csi_{1,15} & csi_{1,16} & \cdots & csi_{1,30} & csi_{2,15} & \cdots & csi_{2,30} & csi_{3,16}^* & csi_{3,15}^* & \cdots & csi_{3,1}^* & csi_{2,16}^* & \cdots & csi_{2,1}^* \\ csi_{2,1} & csi_{2,2} & \cdots & csi_{2,16} & csi_{3,1} & \cdots & csi_{3,16} & csi_{2,30}^* & csi_{2,29}^* & \cdots & csi_{2,15}^* & csi_{1,30}^* & \cdots & csi_{1,15}^* \\ csi_{2,2} & csi_{2,3} & \cdots & csi_{2,17} & csi_{3,2} & \cdots & csi_{3,17} & csi_{2,29}^* & csi_{2,28}^* & \cdots & csi_{2,14}^* & csi_{1,29}^* & \cdots & csi_{1,14}^* \\ \vdots & \vdots & \vdots & \vdots & \vdots & \vdots & \vdots & \vdots & \vdots & \vdots & \vdots & \vdots & \vdots & \vdots \\ csi_{2,15} & csi_{2,16} & \cdots & csi_{2,30} & csi_{3,15} & \cdots & csi_{3,30} & csi_{2,16}^* & csi_{2,15}^* & \cdots & csi_{2,1}^* & csi_{1,16}^* & \cdots & csi_{1,1}^* \end{bmatrix}$$

**Smoothed CSI**<sub>30×64</sub>

Fig. 5. The structure of smoothed CSI matrix.

Finally, we can apply the MUSIC algorithm to the smoothed CSI matrix to estimate the AoA and ToF of each propagation path.

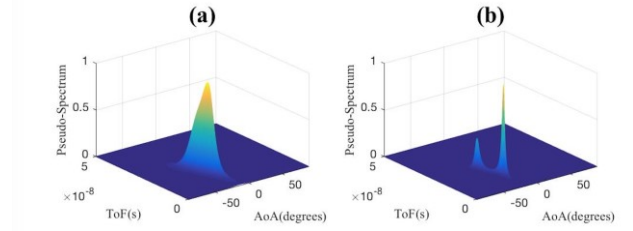


Fig. 6. The results of Simulation 2.

To verify the effectiveness of our proposed algorithm, we conducted another simulation called Simulation 2. Consistent with the condition of Simulation 1, we assumed that there are two coherent signals with similar parameters: AoA  $-20^\circ$ ,  $-30^\circ$  and ToF 10ns, 20ns. Figure 6(a) shows the result of the AoA and ToF estimation with the CSI smoothing proposed by SpotFi. As shown in the figure, the peaks of two propagation paths are merged, making it impossible to estimate the parameters. Encouragingly, when estimating the AoA and ToF of each path with the CSI forward/backward smoothing proposed by this paper, we can distinguish the peaks of the two signals and estimate the AoAs and ToFs.

From Simulation 2, we can preliminarily conclude that the CSI forward/backward smoothing can improve the accuracy of AoA and ToF estimation. In Section 5, we will test the robustness of our approach in reality.

### IV. LOCALIZATION

To achieve localization, besides the joint AoA and ToF estimation, our system includes another three major modules: Direct Path AoA Identification, Range Estimation and Target Localization.

#### A. Direct Path AoA Identification

After we obtain the AoA and ToF of each propagation path by joint estimation as previous, we must pick out the direct path from all propagation paths and get the AoA of direct path. SpotFi employs multiple measurements to determine the most stable path as the direct path. Although high identification accuracy is achieved, this method requires multiple measurements, which is time-consuming and does not guarantee real-time localization.

In our system, we declare the path with the smallest ToF as the direct path from all paths. Although there is a time



synchronization issue on different Wi-Fi cards, the ToFs of all propagation paths include the same delay caused by the Sampling Time Offset (STO) [9] on a single card, hence the ToF of the direct path is still minimal. When we find out the direct path, the AoA corresponding to the direct path is obtained at the same time.

### B. Range Estimation

In order to improve the performance of our system, we use the path loss model [2] to estimate the distance between transceivers based on the Received Signal Strength (RSS) before achieving target localization.

### C. Target Localization

For target localization, we construct a least squares cost function by combining the estimations of direct path AoA and distance from multiple APs represented as follows:

$$\sum_{j=1}^J [(\hat{\theta}_j - \theta_j)^2 + (\hat{d}_j - d_j)^2] \quad (7)$$

where  $J$  is the number of AP,  $\hat{\theta}_j$  and  $\hat{d}_j$  is the estimation of the direct path AoA and distance between the target and the  $j^{th}$  AP,  $\theta_j$  and  $d_j$  is the true value of the AoA and distance between the target and the  $j^{th}$  AP if the target device is actually transmitting at that location. We employ the trust region algorithm to minimize the cost function and obtain the target location finally.

## V. PERFORMANCE EVALUATION AND ANALYSIS

In this section, we will verify the performance of our system through practical experiments and compare it with SpotFi. Our system that was deployed in our laboratory consists of a laptop as target and three desktop computers as APs. Target and APs are all equipped with an Intel 5300 NIC and the Linux CSI Tool [11]. Figure 7 shows the geometry of the test environment, where the blue rectangle indicates the location of the APs, which is known in advance, and the red dot indicates the test location of the target. We selected a total of 16 test points and marked  $L1$  to  $L16$  respectively. In the experiment, the Wi-Fi NICs operate in 5.2GHz Wi-Fi spectrum with 40MHz bandwidth. The target works in injection mode to sending packets, and all APs work in monitor mode to listening packets from the target. Once a packet reaches the AP, a CSI will be obtained through the Linux CSI Tool [11].



Fig. 7. The geometry of the test environment.

To visualize the advantages of the CSI forward/backward smoothing in the joint AoA-ToF estimation, we select the results of  $L16$  and  $L8$  test points as examples. The ground truth AoA of  $L16$  at AP1 is -28 degrees, Figure 8(a) shows the result of the AoA and ToF estimation on  $L16$  at AP1 through the MUSIC algorithm with CSI smoothing, i.e., the SpotFi. There is only one peak in the figure, so we can only identify it as the direct path. According to the position of this peak, the AoA is estimated to be 6 degrees, resulting in an error of 34 degrees compared with the ground truth, which will cause a large error in the final localization stage. However, when we estimate the AoA and ToF for each propagation path on  $L16$  at AP1 through the MUSIC algorithm with CSI forward/backward smoothing, i.e., the proposed, we get satisfactory results. As shown in the Figure 8(b), comparing with the Figure 8(a), we separate this two merged peaks and declare the peak with the smallest ToF as the direct path. The AoA estimation of the direct path is -32 degrees, which reduces the estimation error from 34 degrees to 4 degrees, thus improving the localization performance eventually.

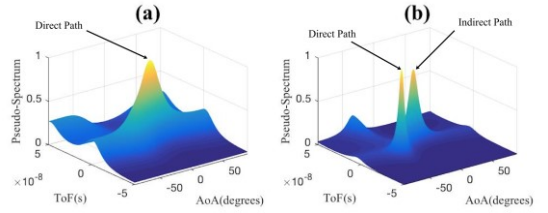


Fig. 8. The result of the AoA estimation of  $L16$  at AP1.

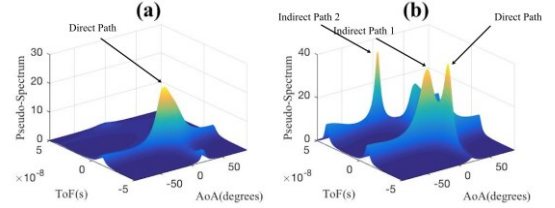


Fig. 9. The result of the AoA estimation of  $L8$  at AP2.

Another example gives similar results. The ground truth AoA of  $L8$  at AP2 is 33 degrees, in the same way, Figure 9 (a) and (b) shows the results of the AoA and ToF estimation through the SpotFi and the proposed respectively. In these two figures, we still declare that the path with the smallest ToF as the direct path, and the angle estimation of the direct path is used as the AoA estimation from the transmitter to the receiver. According to those two figures, the AoA on  $L8$  at AP2 are estimated to be 13 degrees and 28 degrees by the SpotFi and the proposed respectively. Live up to expectations, when using the proposed, we greatly improve the accuracy of the AoA estimation.

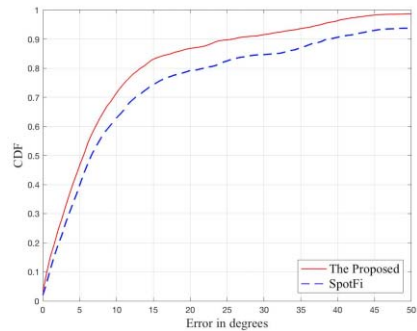


Fig. 10. the CDFs of AoA estimation error by using the proposed and the SpotFi.

For general, we count the results of 16 test points and make the CDFs of AoA estimation error by using the proposed and the SpotFi. As shown in the Figure 10, the median, 60%, 70% and 80% AoA estimation error of the proposed are about 5.5 degrees, 7.2 degrees, 9.5 degrees and 13 degrees respectively, which are all smaller than the SpotFi.

The above experimental results illustrate that the proposed can effectively improve the AoA estimation accuracy of the state-of-the-art AoA-based localization system in complex indoor environments. Intuitively, with a more accurate AoA estimation, the localization accuracy of the system will be better. Next, we will conduct an experiment for indoor localization.

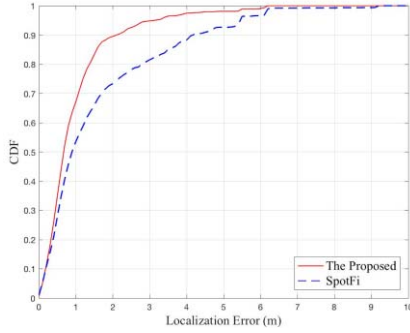


Fig. 11. the CDFs of location error by using the proposed and the SpotFi.

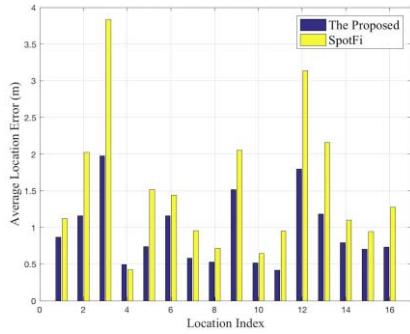


Fig. 12. Comparison chart of the average location error of 16 test points.

To verify the localization performance of our system, we still combined the results of 16 test points and compared with the SpotFi. Figure 11 shows the CDFs of location error by using the proposed and the SpotFi. According to the figure, our system achieves a median localization error of about 0.7m compared with 0.93m for SpotFi, and the 80% localization error of the proposed and the SpotFi are 1.41m and 2.8m respectively. To display more experimental details, we plot the comparison chart of the average location error of 16 test

points in Figure 12, which clearly demonstrate that the proposed can significantly improve the localization accuracy.

## VI. CONCLUSION

This paper proposes the CSI forward/backward smoothing algorithm, which can significantly improve the joint AoA and ToF estimation by using the MUSIC algorithm at low SNRs. Based on the results of experimental, our system can achieve better performance on localization comparing with the SpotFi. Therefore, we believe that our system is robust and stable in a complex indoor environment and can adapt to a variety of indoor localization scenarios.

## REFERENCES

- [1] Manikanta Kotaru, Pengyu Zhang, and Sachin Katti. "Localizing Low-power Backscatter Tags Using Commodity WiFi." In *Proc. ACM CoNEXT '17*, New York, NY, USA, pp. 251-262, 2017.
- [2] P. Bahl and V. N. Padmanabhan, "RADAR: an in-building RF-based user location and tracking system," *Proceedings IEEE INFOCOM 2000. Conference on Computer Communications. Nineteenth Annual Joint Conference of the IEEE Computer and Communications Societies (Cat. No.00CH37064)*, Tel Aviv, vol. 2, pp. 775-784, 2000.
- [3] M.Youssef and A.Agrawala, "The Horus WLAN location determination system," in *Proc. ACM MobiSys '05*, Seattle, WA, pp. 205-218, Jun. 2005.
- [4] S. Sen, B. Radunovic, R. R. Choudhury, and T. Minka, "You are facing the Mona Lisa: Spot localization using PHY layer information," In *Proc. ACM MobiSys '12*, Low Wood Bay, Lake District, United Kingdom, pp. 183-196, Jun. 2012.
- [5] X. Wang, L. Gao and S. Mao, "BiLoc: Bi-Modal Deep Learning for Indoor Localization With Commodity 5GHz WiFi," in *IEEE Access*, vol. 5, pp. 4209-4220, 2017.
- [6] S. Sen, K. K. J. Lee, and P. Congdon, "Avoiding multipath to revive inbuilding WiFi localization," in *Proc. ACM MobiSys '13*, Taipei, Taiwan, pp. 249-262, Jun. 2013.
- [7] R. Schmidt, "Multiple emitter location and signal parameter estimation," in *IEEE Transactions on Antennas and Propagation*, vol. 34, no. 3, pp. 276-280, Mar. 1986.
- [8] J. Xiong and K. Jamieson, "Arraytrack: A fine-grained indoor location system," in *Proc. ACM NSDI '13*, Lombard, IL, pp. 71-84, Apr. 2013.
- [9] Manikanta Kotaru, Kiran Joshi, Dinesh Bharadia, and Sachin Katti. "SpotFi: Decimeter Level Localization Using WiFi." In *Proc. ACM SIGCOMM '15*, New York, NY, USA, pp. 269-282, Aug. 2015.
- [10] Tie-Jun Shan, M. Wax and T. Kailath, "On spatial smoothing for direction-of-arrival estimation of coherent signals," in *IEEE Transactions on Acoustics, Speech, and Signal Processing*, vol. 33, no. 4, pp. 806-811, Aug. 1985.
- [11] D. Halperin, W. J. Hu, A. Sheth, and D. Wetherall, "Predictable 802.11 packet delivery from wireless channel measurements," in *Proc. ACM SIGCOMM '10*, New Delhi, India, pp. 159-170, Sep. 2010.
- [12] S. U. Pillai and B. H. Kwon, "Forward/backward spatial smoothing techniques for coherent signal identification," in *IEEE Transactions on Acoustics, Speech, and Signal Processing*, vol. 37, no. 1, pp. 8-15, Jan. 1989.